Synthesis of High-Quality Metal Sulfide Nanoparticles from Alkyl Xanthate Single Precursors in Alkylamine Solvents

Narayan Pradhan,[†] Beni Katz,[†] and Shlomo Efrima*[,†,‡]

Department of Chemistry and the Ilse Katz Center for Meso and Nanoscale Science and Technology, Ben Gurion University of the Negev, Beer-Sheva, 84105, Israel

Received: June 24, 2003; In Final Form: September 24, 2003

A synthesis of various metal sulfide nanoparticles at relatively low temperature with use of a single precursor under ambient conditions is described. Metal alkyl xanthates (as well as thiocarbamates and thiocarbonates) are used as the precursor. Lewis base alkylamine solvents promote the reaction at low temperatures (from below room temperature up to ∼150 °C). By this method we form crystalline particles which are size- and shape-tunable and are usually monodiserse. This tunability is achieved by controlling parameters such as the reaction temperature, the reaction time, the concentration of the precursor, and the alkyl chain length. Core/shell structures are synthesized with the same method, using the same precursors, applying either a single-step or a dual-step process. CdS spherical particles, for instance, exhibit a narrow (∼30 nm fwhm) tunable excitonic fluorescence, and a broad, long wavelength defect emission, which intensity can be adjusted in a controlled manner, and even totally eliminated. Quantum yields of these particles are ∼2% for the "bare" particles and ∼16% for the ZnS-shelled, annealed particles. A short-wavelength (390−420 nm) narrow (30−35 nm fwhm) excitonic emission is observed for ZnS/CdS structures.

1. Introduction

In recent years fluorescing semiconductor nanoparticles (quantum dots) have attracted considerable attention, mostly due to their size-dependent tunable spectroscopic properties.[1−3] Currently fluorescing (CdSe) particles are put to use as biological labels alongside, or even replacing, fluorescing molecular probes.[4−9] They are characterized by very narrow and tunable (excitonic) emission bands and long-range stability even under illumination. At times, their photoluminescence (PL) is dominated by a much broader surface defect emission at longer wavelengths. This emission can be removed by surface passivation of the particles—capping by various organic molecules or shelling with a higher band gap semiconductor coating—resulting in high quantum yields of the excitonic band.[10−16]

Solution colloidal methods provide a most efficient pathway for the synthesis of chalcogenide quantum dots, where particles are first nucleated and then grown to a desired size by a controlled reaction of precursor molecules. The currently most widely used method, yielding tightly controlled, monodisperse, high-quality, crystalline particles, involves reactions of the metal ion (i.e. Cd^{2+}) source and a molecule containing the chalcogenide (sulfur, selenium, etc.) in a complexing solution of trioctylphosphine (TOP) in trioctylphosphineoxide (TOPO).[17−21] This synthetic method requires high temperatures (200−350 °C) and uses air-sensitive and highly poisonous reagents, thus requiring a strictly air-free atmosphere. The recent introduction of CdO as one of the precursors improves this situation.[22] Yu and Peng[23] synthesized high-quality CdS particles using CdS in a noncoordinating solvent octadecene with oleic acid as stabilizer. Very recently Joo et al.[24] reported an interesting generic method for the synthesis of metal sulfides using oleylamine as a stabilizer.

Extensive pioneering work by O'Brien et al. demonstrated that less hazardous precursors can be used (metal salts of ethylxanthates and dialkylthiocarbamantes), though the TOP/TOPO high-temperature environment was still employed to obtain crystalline, defect-free particles.[25−34] The fluorescence spectra of some of these particles exhibit a ∼40−50 nm fwhm excitonic emission band of unspecified quantum yield. It is not clear whether the spectrum is tunable nor whether there is a long wavelength emission, since the PL spectra they usually present do not extend beyond 500 nm.

Lower temperature, convenient microemulsion-based methods have also been developed[35,36] but these generally yield particles of much lesser quality with a wider size distribution, often exhibiting predominately the long wavelength, broad, not tunable, defect (deep-trap) emission.

Recently we introduced a new method for synthesizing metal sulfide particles of high quality utilizing a Lewis-base catalyzed, low-temperature thermal decomposition of various single precursors of metal alkyl xanthates[35] (Scheme 1). Alkylamine is used as the solvent to promote the decomposition, and it also acts as a stabilizing agent for the particles that form. Despite the low reaction temperature, the particles are crystalline, defect-free, and of a well-defined and easily tunable narrow size distribution, exhibiting intense, narrow, and tunable excitonic emission. We recently demonstrated the utility of our method for producing CdS particles and briefly mentioned CdS/ZnS, core/shell particles.[37]

Here we present a detailed study of spherical and nonspherical MS particles (M = Cd, Zn, Pb, Hg, Ni, Cu, Mn), emphasizing what we believe are core−shell CdS/ZnS and ZnS/CdS nanoparticles. The particles are tunable with respect to their size and their optical properties. We describe a novel, single-pot method for the production of ZnS/CdS, core/shell structures, whereby all the reagents (for the core and for the shell) are loaded together, using a simple temperature protocol to initialize the

* Address correspondence to this author. E-mail: efrima@bgumail.bgu.ac.il.
[†] Department of Chemistry.
[‡] Ilse Katz Center for Meso and Nanoscale Science and Technology.

10.1021/jp035795l CCC: $25.00
Published on Web 11/20/2003

SCHEME 1

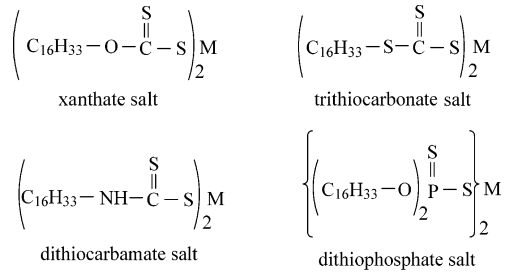

production of the core, and followed at a proper time by the formation of the shell. We also describe an alternative stepwise synthesis consisting first of production of a ZnS core and then, in a second separate stage, a CdS shell.

We also describe here the use of reaction time, temperature, and/or concentration control to achieve size (and spectroscopic properties) tunability of the particles. Temperature and concentration control also provide a means to obtain various shapes (spheres, rods, etc.). The methods we introduce, based on reactions of metal xanthates (as well as thiocarbamates and thiocarbonates), are general and work equally well for the production of many other metal sulfide particles, such as HgS, PbS, CuS, NiS, and MnS. Furthermore, at times, such as for HgS and PbS, these reactions can be carried out at or even below room temperature, where nevertheless crystalline particles form. This demonstrates the capability of obtaining crystalline nanostructures at low temperatures, contrary to common experience to date.

2. Experimental Section

2.1. Chemicals and Instrumentation. Hexadecylamine (HDA), tetradecylamine (TDA), trioctyl phosphine (TOP), trioctyl phosphineoxide (TOPO), trioctylamine (TOA), dodecylamine(DA), cadmium chloride, cadmium perchlorate, zinc nitrate, lead nitrate, mercuric nitrate, nickel sulfate, manganese sulfate, and copper nitrate were purchased from Aldrich. All are used as such without further purification. Perylene was purchased from Sigma and potassium alkyl xanthates, dithiocarbamates, and trithiocarbonates were synthesized with known methods.[36−38]

Water is of 18 MΩ cm resistivity, from a Barnsted E-pure water purifier.

UV−visible spectra are recorded with a 8452A HP diode array spectrophotometer in the range 190−820 nm, with a resolution of 2 nm. Fluorescence is acquired with Jobin Yvon Fluorolog-2. Transmission electron microscopy is carried out with a JEOL 2010 HR-TEM, equipped with a Gatan multiscan CCD camera. Energy-dispersive X-ray spectroscopy (EDS) is performed by using an Oxford linked ISIS 6498 (version 1.4). A typical accelerating voltage of 200 kV is used with magnifications of ×100 000 for obtaining size distributions, and ×600 000 for single-particle analysis. A drop of a suspension of the colloid in dichloromethane is placed on a Lacey carbon-Formvar, 300 mesh copper grid (Ted Pella 01883-F) and allowed to evaporate.

2.2. Synthetic Procedures. *2.2.1. Synthesis of Metal Xanthates, Dithiocarbamates, Trithiocarbonates, and Dithiophosphates.* A 0.1 M aqueous solution of the corresponding metal salt is added dropwise with stirring into 10 mL of a 0.05 M potassium xanthate methanolic (or aqueous for ethylxanthate) solution. The metal xanthate forms rapidly and precipitates. New precipitation ends when a 1:2 metal-to-xanthate molar ratio is reached indicating that a dixanthate forms. We usually add a little excess (one drop) of the metal salt solution to ensure complete conversion to the metal xanthate. The mixture is centrifuged and washed several times with a water/methanol mixture (1:3) and finally with methanol. The resulting metal dixanthates are dried at room temperature and can be stored for weeks. The dixanthate showed by elemental analysis a C 54.19% and H 8.70% content, compared to 54.7% and 8.8%, respectively, expected of the cadmium dixanthate. Dithiocarbamates, trithiocarbonates, and dithiophosphates are formed similarly, except that a solution of their potassium salt is prepared in hot methanol and their cadmium salts are prepared as methanolic solutions of $CdClO_4$ or $CdCl_2$.

2.2.2. Synthesis of CdS and ZnS Spherical Particles. CdS particles are synthesized with ethyl, decyl, and hexadecyl xanthates and the hexadecyl analogues of the thiocarbamate and -carbonate precursors. HDA (2 g, 0.0083 mol) in a clean and dry test tube was melted and then kept at 50 °C. At this temperature ∼1.6×10^{-4} mol of the metal xanthate precursor was added with stirring. When a clear and homogeneous solution formed the temperature was raised to the desired reaction temperature, monitoring the product by fluorescence. For Cd and Zn xanthates, the decomposition reaction temperature in HDA was in the range 70−120 °C, with subsequent annealing performed at 120−140 °C. For trithiocarbonate, the decomposition reaction temperature in HDA is higher, 125 °C to 150 °C, and annealing was carried out at ∼170−200 °C. The dithiocarbamate metal salt decomposed in HDA at an even higher temperature, 170 °C, and was annealed at 200 °C. After annealing, the temperature was reduced to 70 °C and methanol was added to flocculate the particles. The deposit was washed several times with absolute methanol and dried at room temperature.

2.2.3. Synthesis of CdS Rods. To 0.0083 mol of melted HDA, we add an equal weight of Cd hexadecylxanthate (Cd−HDX). This was more than 10-fold higher concentration of Cd−HDX compared to the previous procedure used for production of predominately spherical particles. The solution was kept at 50 °C for 30 min until complete dissolution took place. At this stage the temperature was increased to 120 °C for another 30 min to allow the decomposition reaction to occur. At this temperature (and concentration) rods were formed, rather than spheres. The solution turned orange, then red, and ended up brown. Finally an additional 0.003 mol of melted HDA at 120 °C was added to prevent agglomeration, and annealing was carried out at the same temperature for another 60 min. The solution was cooled gradually under ambient conditions. The CdS rods were collected by centrifugation after methanol was added at 70 °C for flocculation. (ZnS rods and wires form when using a 10-fold higher concentration of zinc hexadecylxanthate-was used or when the hexadecylxanthate was replaced by ethylxanthate.)

2.2.4. Synthesis of PbS and HgS Particles. Xanthates of Pb^{2+} and Hg^{2+} in a primary amine (such as decylamine, DA) decomposed already at room temperature. Consequently, it was difficult to prepare a homogeneous solution of these metal xanthates in HDA (which melts at 45 °C) prior to the reaction itself. We therefore prepared a solution of the metal xanthate in a tertiary amine (trioctylamine, TOA) (CCl_4 can also be used) and then added it to DA at room temperature. For example, 1.2×10^{-4} mol of lead hexadecyl xanthate were dissolved in 3×10^{-4} mol of TOA and the solution was stirred and sonicated at room temperature for 30 min to obtain a homogeneous solution.

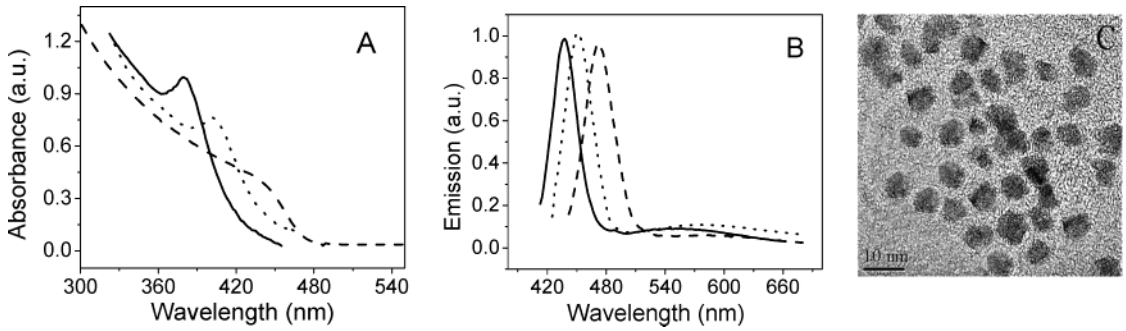

Figure 1. (A) UV−visible absorption and (B) the corresponding PL spectra of colloidal CdS particles excited at 370 nm formed within 20 (full line), 50 (dotted line), and 90 min (broken line) of the reaction, at 125 °C; (C) TEM micrograph of the CdS particles (90 min reaction time).

This solution was added to 1×10^{-3} mol of DA and the particles formed at room temperature. The solution was annealed at 80 °C and collected by flocculation with methanol.

2.2.5. Synthesis of CuS, NiS, and MnS Particles. Primary amines displaced the xanthate from Cu, Ni, and Mn HDX, as evidenced by an appearance of a green color upon dissolution (for Cu and Ni, Mn). In that case heating the solution even up to 200 °C did not produce any sulfide particles. We therefore used a weaker ligand such as tertiary amine solvents to synthesize the Cu, Ni, and Mn sulfide particles. Metal xanthates (1.2×10^{-4} mol) dissolved in 1.5 mL of trioctylamine were heated to 150 °C to compensate for the weaker activity of the tertiary solvent. After formation of the particles the temperature was decreased and HDA was added to replace the tertiary amine as the capping agent at 70 °C. The product was annealed at 160 °C and collected by flocculation with methanol at 70 °C.

2.2.6. Two-Stage Synthesis of CdS/ZnS Core−Shell Nanoparticles. Annealed CdS particles produced in HDA (synthesized as described above from 8.1×10^{-5} mol of Cd HDX in 6.6×10^{-3} mol of HDA) were redissolved in HDA at 120 °C to serve as cores. About one-half of a HDA solution of Zn−HDX (1.7×10^{-4} mol, 0.12 g, Zn−HDX in 4.4×10^{-3} mol, 1 g, of HDA) was added at 60 °C to the CdS core dispersion. A heated dropper was used to avoid solidification of the Zn−HDX in the HDA solution during transfer. The temperature was then stepped up at a rate of 10 °C per 10 min. When 150 °C was reached the sample was cooled back to 60 °C and the remaining portion of Zn−HDX in HDA was added, repeating the gradual increase of the temperature. We added the shelling reagent in portions, to maintain a low concentration, to minimize the probability of its decomposition in the bulk of the solution forming separate ZnS particles, rather than shelling the CdS cores. The gradual temperature increase was used also for that very same purpose. Finally the temperature was set to 170 °C for annealing and the product was flocculated at 70 °C with methanol. The flocculated solid was washed several times with methanol and dispersed in toluene. We believe that core/shell structures form rather than mixed particles, as discussed later.

2.2.7. Two-Stage Synthesis of ZnS/CdS Nanoparticles. One can use the same two-stage procedure described above for the production of CdS/ZnS particles, switching the Zn and the Cd, to obtain ZnS/CdS structures.

2.2.8. One-Pot "Simultaneous" Synthesis of Core/Shell ZnS/CdS Particles. This is a novel method to produce plausibly core/shell structures almost in one stroke. We used Zn−HDX as the source of ZnS cores (decomposes in HDA at 70 °C) and Cd−HDC as the source for the CdS shell (decomposes in HDA only at a higher temperature, ~170 °C). Zn−HDX (0.05 g, 7.14×10^{-5} mol) and Cd HDC (0.05 g, 7.12×10^{-5} mol) were loaded in 2 g (8.8×10^{-3} mol) of HDA at 60 °C under a flow of nitrogen (for safety). The temperature was slowly increased (a 10-min wait for each 10 °C temperature increase) up to 200 °C. First the Zn−HDX reacted and only later, at a higher temperature, did the Cd−HDC decompose and form CdS. The Cd−HDC starts to react already at 120 °C but the reaction is confined to the surface of the ZnS cores, as in solution a much higher temperature (170 °C) is required to form CdS from Cd−HDC. The reaction was monitored periodically by fluorescence. Finally the temperature was decreased to 70 °C, and methanol was added to collect the HDA-capped particles. The same procedure works similarly with the ethylxanthate salts.

2.3. Determination of the PL Quantum Yield, QY. This was carried out by using perylene as the reference with a known QY of 70% (at 412-nm excitation).[31] We first determined the QY of the particles at 412-nm excitation, and then used this value for evaluating their QY at 370-nm excitation using the following relationship.

$$\mathrm{QY}_{370\mathrm{nm}} = \mathrm{QY}_{412\mathrm{nm}}\left[\frac{I_{\mathrm{PL}(370\mathrm{nm})}}{I_{\mathrm{PL}(412\mathrm{nm})}}\right]\left[\frac{\mathrm{OD}_{370\mathrm{nm}}}{\mathrm{OD}_{412\mathrm{nm}}}\right]\left[\frac{R_{\mathrm{s}(412\mathrm{nm})}}{R_{\mathrm{s}(370\mathrm{nm})}}\right]\left[\frac{412}{370}\right]^4 \quad (1)$$

I_{PL} is the measured fluorescence intensity (at the corresponding wavelength), OD is the absorption optical density, and R_{s} is the intensity of the Raman bands of the solvent. The third term, involving the ratio of OD's, corrects for the wavelength-dependent degree of excitation. The fourth term (involving the Raman intensity of the solvent bands) approximately accounts for the different absorption of the exciting light in the media at the two wavelengths, as well as for the differences in the exciting light intensity. The last term normalizes the Raman signals with respect to the wavelength.

3. Results and Discussion

3.1. Formation of Metal Sulfide Particles from Metal Xanthates. Tunability of fluorescing CdS particles from Cd HDX can be readily achieved by controlling either of the following experimental conditions: the concentration of the precursors, the reaction time, or the reaction temperature. Further tunability can be obtained simply by changing the length of the alkyl chain of the xanthate. Thus these methods are highly versatile and offer a large measure of control over the products. In our previous work[35] we have demonstrated size and optical tuning of CdS particles by controlling the reaction temperature. Here we show how other parameters can be employed for the same purpose.

Figure 1 shows the effect of the reaction time on the UV−visible absorbance and the PL spectra of CdS particles formed from Cd−HDX. The precursor Cd−HDX is dissolved in HDA

TABLE 1: Crystal Plane Spacings of Different Metal Sulfides from Electron Diffraction Measurements

metal sulfides	main crystal plane spacing (Å)		
	measurements	literature[45]	ticket no.[45]
CdS	3.352, 2.086, 1.762	3.364, 2.058, 1.753[37]	10-0454
ZnS	3.134, 2.957, 1.91, 1.764	3.129, 2.925, 1.91, 1.764[46]	36-1050
PbS	2.961, 3.481, 2.011	2.969, 3.429, 2.099	05-0592
MnS	2.614, 1.844, 1.480	2.612, 1.847, 1.50	06-0518
CuS	2.798, 1.905, 3.004	2.813, 1.896, 3.048	06-0464
NiS	2.951, 2.592, 1.971, 1.723	3.01, 2.608, 1.845, 1.57	27-0343
HgS	3.492, 2.908, 1.998	3.378, 2.926, 2.068	06-0261

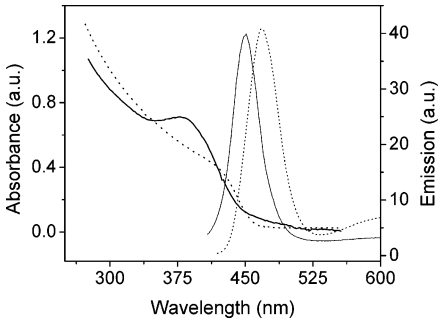

Figure 2. UV−visible absorption (left) and PL spectra excited at 370 nm (right) of the 1:50 (full line) and 1:10 (dotted line) weight ratio of Cd−HDX and HDA. The reaction was carried out at 90 °C for 30 min and annealed at 130 °C for 90 min.

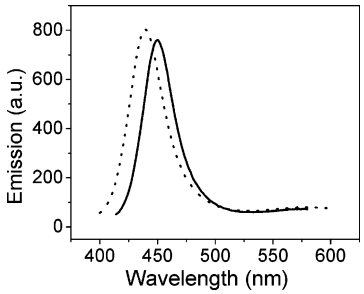

Figure 3. PL spectra of CdS particles formed by decomposition of Cd-EX (dotted line) and Cd−HDX (full line). Excitation at 370 nm.

below 70 °C and the temperature is immediately increased to 130 °C. At this temperature the reaction is much faster than at 70 °C. Annealing takes place simultaneously with the production of the particles, as evidenced by the very low intensity of the long wavelength emission in Figure 1 and the further decrease of this weak emission with reaction/annealing time.

The reaction is terminated by lowering the temperature to 70 °C and flocculating the particles with methanol. The two emission bands seen in the PL spectra are the well-known excitonic transition (the narrow band at the shorter wavelengths) and the broad emission at longer wavelengths associated with surface traps (defects).[37,42−44]

Both absorption and emission spectra exhibit a gradual red-shift of the excitonic spectral features with time, as expected from gradually growing nanoparticles when wave function confinement is significant. The sharp absorption peaks for the particles harvested at shorter times, compared to the somewhat broader feature seen at long reaction times, are also in agreement with this conclusion. Some of the particles are spherical, but some are faceted or aggregated. Electron diffraction shows the CdS particles are crystalline with the wurtzite structure (Table 1).

A similar control can also be achieved by varying the concentration of the metal xanthate precursor keeping other reaction conditions unaltered (Figure 2).

Finally, as stated above, one can achieve further control by varying the alkyl chain length of the xanthates. We demonstrate this by a comparison between the reactions of cadmium ethylxanthate, Cd−EX, and hexadecylxanthate. Cadmium ethylxanthate by itself decomposes at 160 °C,[47] compared to 145 °C for cadmium hexadecylxanthate.[37] In HDA, however, both decompose well below 100 °C, while cadmium ethylxanthate exhibits faster nucleation and growth.

Figure 3 shows the fluorescence spectra obtained by separately decomposing Cd−EX and Cd−HDX in HDA at 130 °C (to obtain simultaneous annealing). Both spectra are taken for equal reaction times. Note that CdS produced from ethylxanthate is blue-shifted compared to the particles obtained from the hexadecylxanthate precursor under similar reaction conditions. This suggests that indeed Cd−EX nucleates faster than Cd−HDX, and therefore yields a larger number of smaller particles.

Direct evidence to the faster reaction of the EX precursor is seen by the following observation. In the course of the reaction (for either Cd−EX and Cd−HDX) the PL spectra tend to red-shift with time (Figure 1 for HDX). However, under similar experimental conditions (130 °C reaction temperature and the same precursor molar concentration), the PL of the particles produced from Cd−EX stops changing within 20 min, while the spectrum of the product of Cd−HDX decomposition still shifts for up to 90 min.

As we discuss below, the decomposition of Cd−HDX xanthate involves evolution of OCS as a gas at the reaction temperature. Cd−EX should also release ethylene. Thus, the EX reaction might be faster because stirring by the evolving gas might be more effective in bringing sufficient precursor molecules to a close proximity to react, in addition to any specific effect of the alkyl chain.

The high (spectroscopic) quality and the control of the particles produced by decomposition of the metal xanthates in HDA are strongly determined by this specific class of amine solvents, which drive the reaction at low temperatures. When the metal xanthate decomposition is carried out at higher temperatures, above its intrinsic thermal decomposition temperature, we cannot obtain tunability of the excitonic absorption or emission. For example, reacting cadmium ethylxanthate above 160 °C (in HDA), the excitonic band fully develops within a very short time from the beginning of the reaction (∼2 min) and does not shift any more. One virtually loses control via the reaction time. Furthermore, while the high-temperature decomposition gives particles with both the excitonic and the surface trap PL, at lower temperatures, in the HDA driven route (with reaction and annealing at ∼125 °C), only the excitonic emission is observed. Figure 4 shows a comparison of the emission spectra obtained when the reaction is carried out at 125 °C (below the self-decomposition temperature) and at 190 °C (well above that temperature). Note that the excitonic emission of the "high-temperature" particles is broader than that for those produced at the lower temperature (43 nm compared to 37 nm, fwhm), indicating a tighter size distribution at low temperature. It is also red shifted at the high temperature, suggesting that

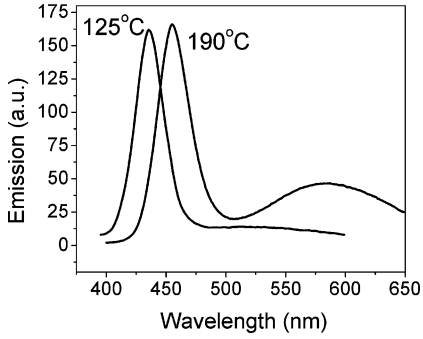

Figure 4. PL spectra of CdS particles formed from Cd−EX decomposed at 125 (left) and 190 °C (right). Excitation at 370 nm.

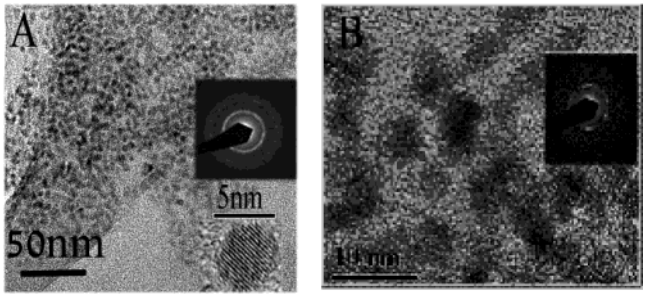

Figure 5. TEM micrographs of CdS, synthesized from Cd−HDC (A) and Cd−HDTTC (B). The reaction temperature was 180 °C and annealing was carried out at 200 °C.

there are larger particles, probably due to a smaller nucleation/growth rate ratio, despite the higher temperature. The "high-temperature" particles also exhibit a very significant long wavelength, defect emission, which cannot be removed by annealing, even at ∼220 °C and under rigorous inert atmospheric conditions. This comparison highlights the essential role of the amine solvent in the production of the particles and in determining their properties.

3.2. Formation of Metal Sulfide Particles from Metal Dithiocarbamates or Trithiocarbonates. Similarly to xanthates, dithiocarbamates or trithiocarbonates might also serve as potential sulfur sources for a single-precursor synthesis of metal sulfide particles. It turns out that these compounds require higher temperatures for decomposition of the respective metal salt, even in an amine solvent. In addition, and perhaps related to the necessary higher reaction temperatures, the quality of the particles is inferior to those formed from xanthates. We find, for instance, that even though particles do form from Cd−HDC above 140 °C (Figure 5A) or from Cd−HDTTC above ∼125 °C (Figure 5B), they are associated with significant deep trap long wavelength surface defect emission and an insignificant excitonic emission (Figure 6). The emission depends on the reaction temperature: the weak excitonic and the dominating broad long wavelength features seem to red-shift with temperature.

We attribute the shifts more to changes in shape than to simple quantum confinement size effects, especially for the defect emission. The change in the spectra is especially noticeable when the reaction temperature is elevated from 140 °C to above the self-decomposition temperature (170 °C for HDC). At the lower temperature (where the solvent has a more significant role in controlling the reaction) the absorption spectrum still exhibits a sharp feature reminiscent of a narrow size distribution of small particles. The broad surface emission peaks at ∼570 nm, similar to what is seen in "good", though un-annealed CdS particles. At the higher reaction temperatures the absorption spectra are smooth with smeared features and

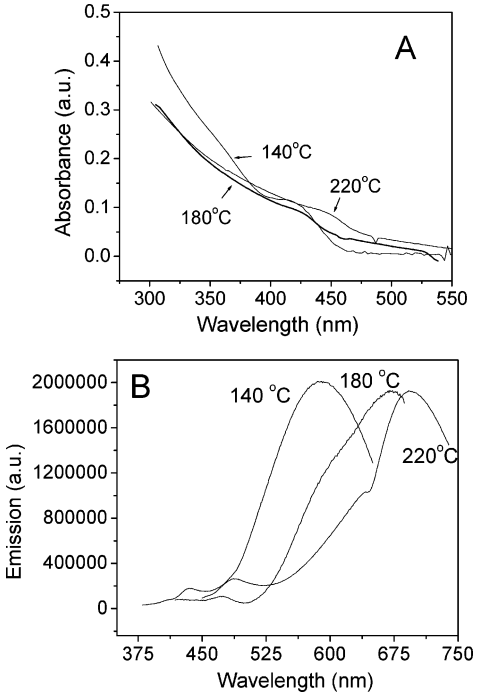

Figure 6. UV−visible absorption spectra (A) and the corresponding PL spectra excited at 370 nm (B) of CdS particles formed from Cd−HDC at different temperatures.

the broad defect emission is strongly shifted to 650−750 nm. The weak PL bands do not show typical confined excitonic character, but rather are more similar to the bulk band edge emission. The particles are stable even when kept for 2 h at 200 °C (the solution remains yellow), but above 250 °C the suspensions turn orange red, probably due to a change in the shape of the particles (see below).[48]

The apparent inferior behavior of the dithiocarbamate and the trithiocarbonates probably is an intrinsic property of these ligands, compared to xanthates, as suggested by the intrinsically higher temperature required for their decomposition. The related dialkyldithiophosphates turn out to be totally unreactive in producing cadmium sulfide. However, it is still possible that in combination with a stronger liganding solvent or for other metals (such as mercury and lead) these precursors might be useful for the production of the sulfide particles.

Notwithstanding the above, even at present, dithiocarbamates and trithiocarbonates still have a useful role in the production of core/shell structures in a single pot manner, as will be demonstrated in a later section of this report. In that context we utilize their higher decomposition temperatures for their use as shelling precursors that readily deposit on metal sulfide cores even at lower temperatures, while they do not form their own separate particles in solution.

3.3. Shape Control of CdS Particles. Besides the size, the shape of the particles can also be modified by varying the reaction temperature, the precursor concentration, or the reaction time. Reacting Cd−HDX below 125 °C and at low precursor concentration (∼1:20 of Cd−HDX:HDA wt ratio) initially yields spherical particles. Typical conditions for this are the following: reacting Cd−HDX in HDA at 125 °C for 90 min, or reacting for 30 min at 90 °C (to decompose first most of the precursor) and then annealing at 125 °C[35] (Figure 7A). However, the particles acquire an elliptical shape either at longer reaction times (>180 min at 125 °C) or at higher temperature (>90 min at 140 °C, Figure 7B).

The emission spectra remain similar to that of the spherical particles. Keeping the particles at 160 °C for longer times (∼250

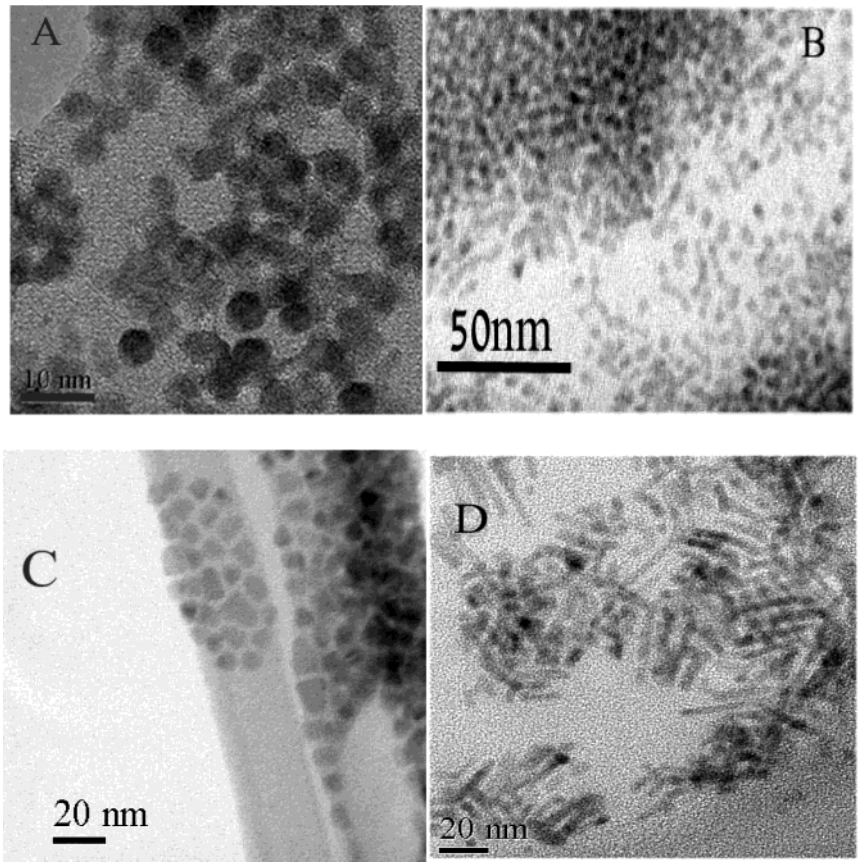

Figure 7. TEM micrographs of CdS particles of different shapes produced from Cd−HDX, using different reaction conditions: (A) 1:20 molar ratio of Cd−HDX and HDA, annealed at 125 °C for 90 min (B) 1:20 molar ratio of Cd−HDX and HDA, annealed at 140 °C for 210 min, (C) 1:20 molar ratio of Cd−HDX and HDA, annealed at 160 °C for 150 min, (D) 1:3 molar ratio of Cd−HDX and HDA, annealed at 125 °C for 90 min.

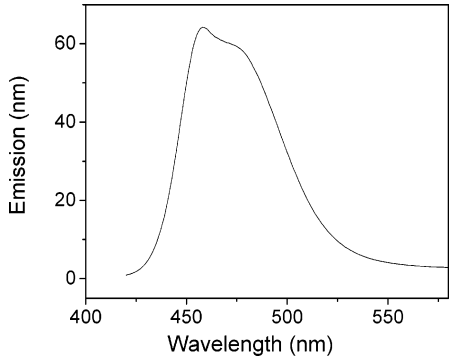

Figure 8. PL spectrum of polygonal CdS particles (excitation at 370 nm).

min), an additional change into a polygonal, facetted shape occurs (Figure 7C). The PL spectrum of these polygonal particles shows a broad and split peak (at ∼460 and ∼475 nm) (Figure 8). Interestingly, when decomposing cadmium xanthate (EX, for instance) at a temperature above that of the decomposition of the pure solid, only spherical particles are formed even under prolonged heating. Apparently at the high temperatures the particles form almost at once having statistically favorable spherical shapes, while at lower temperatures there is a much slower growth stage succeeding the nucleation, allowing for some directional growth selectivity.

The shape of the particles is controlled by the concentration of the precursor as well. At high concentrations (∼1:1 Cd−HDX:HDA wt ratio) CdS rods (∼5 nm width and ∼20 nm length) are preferentially formed at 125 °C (Figure 7D). Thus one can conveniently control size and shape by changing the parameters. This preference to rods in the presence of excess precursor might be related to the appearance of elliptic particles upon heating of low-temperature nucleated CdS particles (see above) when a clear separation between nucleation and growth takes place.

3.4. Sulfides of Other Metals. The same single precursor method can be used to produce various other metal sulfide particles. Crystalline (Table 1) ZnS particles are easily formed with Zn xanthates, such as EX and HDX. Similar to the analogous cadmium reactions, HDA strongly lowers the decomposition temperature for the formation of ZnS particles (to ∼70 °C). Figure 9 shows the UV−visible spectrum and TEM of ZnS particles synthesized from Zn−HDX at 90 °C (annealed at 150 °C for 90 min). The expected shift of the UV−visible spectrum from 270 nm to 300 nm is observed upon an increase in the size of the particles, demonstrating quantum size tunability**.** The emission spectra are dominated by a weak defect band centered at 440 nm, as is common for ZnS, and not shown here. TEM shows that the particles (with maximum absorbance at 300 nm) are uniformly ∼4.5 nm in diameter.

Hg and Pb xanthates decompose instantaneously in melted HDA (at ∼50 °C), even before they form a homogeneous solution. These xanthates produce metal sulfide particles in DA even when decomposed at room temperature. Hence the less reactive tertiary amine (TOA) is chosen to dissolve the metal xanthate. When this solution is added to DA at room temperature, metal sulfides are formed instantaneously. Annealing is carried out at 70 to 90 °C for 90 min. The TEM of HgS and PbS shows disk and octagonal particles, respectively, on the 20 nm scale range (Figure 10). Highly crystalline structures are obtained, as evidenced especially for Pb. The diffraction patterns (Table 1) confirm the regular crystal structure of HgS and PbS.

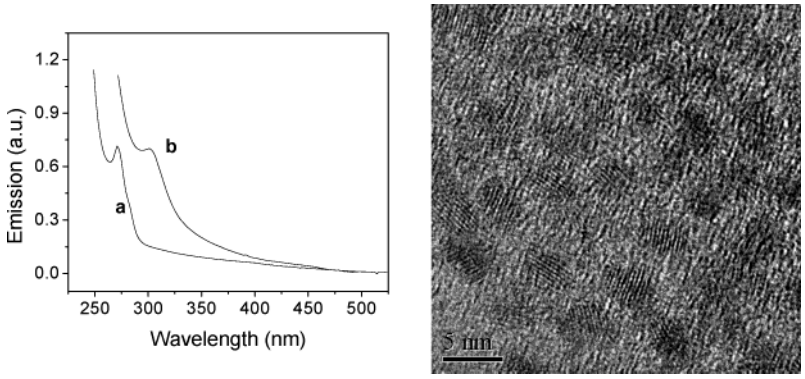

Figure 9. (Left) UV−visible spectra of ZnS colloidal particles synthesized from Zn−HDX at 90 °C (annealed at 150 °C). Curves "a" and "b" show the spectrum after 10 min of reaction and after 140 min of reaction followed by annealing, respectively. (Right) TEM of ZnS particles (of curve "b").

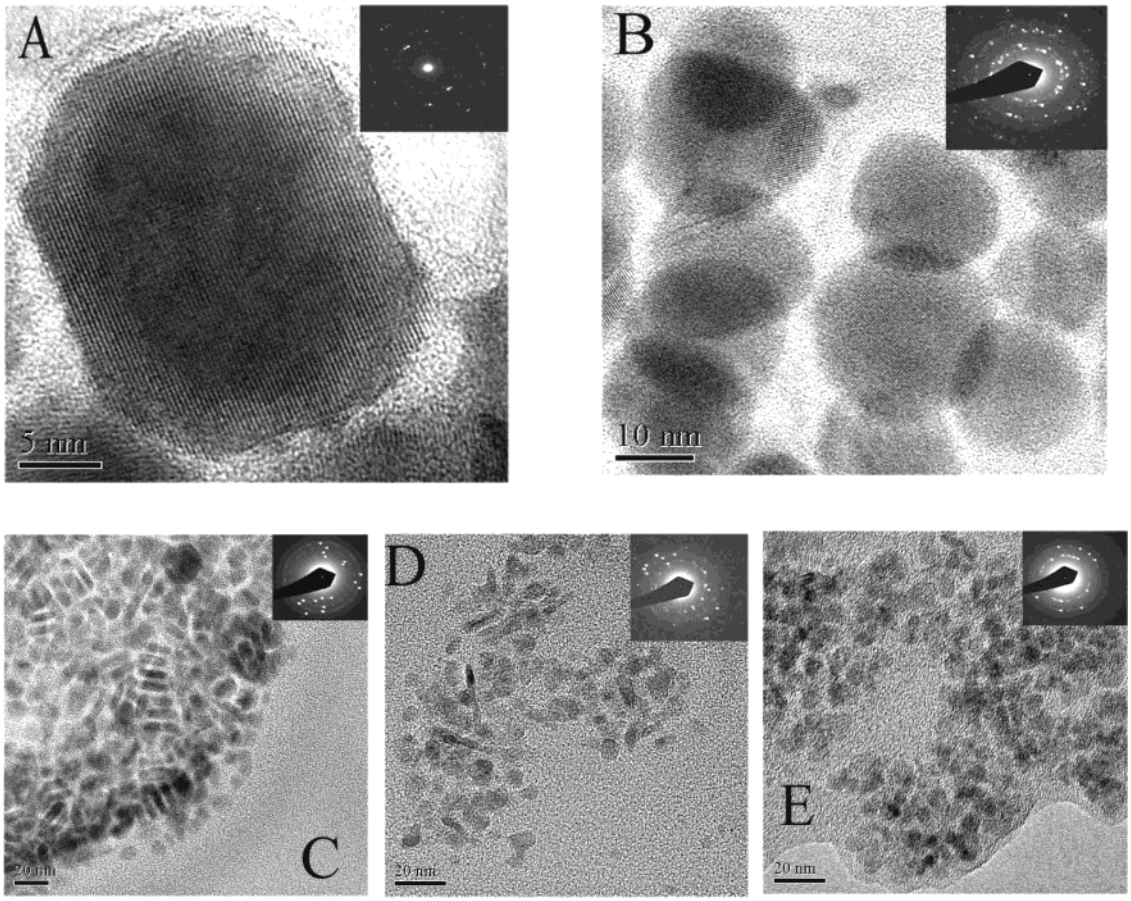

Figure 10. TEM micrographs of PbS (A), HgS (B), CuS (C), NiS (D), and MnS (E) particles. The corresponding diffractograms are included in each frame.

We believe that size and shape control for HgS and PbS might be achieved in chilled solutions or by employing a single short-temperature burst for nucleation followed by low-temperature growth. Work in these directions is planned.

Cu, Mn, and Ni sulfide particles are produced as described in the Experimental Section. The main problem with these metals is to overcome the replacement of the xanthate by the solvent, such as HDA. To prevent this, weaker ligands, such as tertiary amine solvents, are used. TEM (Figure 10) shows for CuS and NiS a mixture of rods and spheres while MnS appears as faceted particles, under the reaction conditions we used. Table 1 shows the good correspondence with known crystal structures of these sulfides. Nickel sulfides are known to form a variety of nonstoichiometric crystals. The closest fit we could find for nickel sulfide was with $Ni_{3-x}S_2$ (with x close to 0), but we cannot presently pinpoint the precise composition. We plan to explore soon the conditions required to produce particles of CuS, NiS, and MnS of various given shapes or sizes.

3.5. The Role of the Solvent and the Mechanism of Decomposition of the Metal Xanthates. The alkylamine solvents we use have a central role in the synthesis of the particles from the metal xanthate precursors. First and foremost, their role is apparent in the significant lowering of the decomposition temperature of the metal alkyl xanthates from above 140 to 70 °C and for alkyl dithiocarbamates from 170 to 125 °C, while no such effect was observed for the alkyl trithiocarbonates (or, for that matter, dialkyl dithiophosphates).

Other solvents, such as trioctylphosphine, alkylthiols, or secondary and tertiary alkylamines (instead of HDA), also have some effect on the reaction. However, most of these solvents

SCHEME 2: The Chugaev Reaction (top) and Chugaev-like Mechanism for the Decomposition of Cd−Xanthate (bottom).

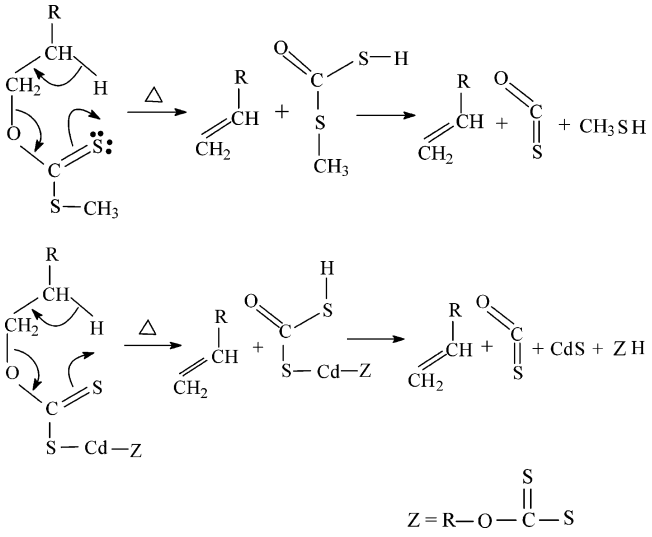

are less effective compared to the primary alkylamines in terms of the reaction temperature, or the necessary reaction time, or the quality of the product particles. For instance, in TOP, the formation of CdS particles occurs at room temperature; however, it is a very slow process and hours are needed to complete the reaction. When the widely used solvent TOPO is employed the decomposition temperature remains as high as for the metal xanthate itself. We observe formation of ~4.8 nm (by TEM) CdS particles from Cd−HDX in TOPO, starting only at 150 °C. In addition, we cannot achieve any tunability by controlling the temperature, and the excitonic emission appears at a constant wavelength of 475 nm. A similar result was also reported by O'Briene. et al. for Cd−EX.[48]

The effect of the solvent might be understood on the basis of the molecular mechanism of the decomposition reaction (supposedly related to the Chugaev reaction)[49] (Scheme 2). This reaction involves a concerted three electron-pair shift. Eventually OCS is released and an olefin is formed. We suggest that the cadmium dixanthate decomposes similarly via a concerted shift of the same three electron pairs, catalyzed by the solvent (Scheme 3). The solvent might perhaps have a 4-fold role.

First, the solvent might activate the $O-C-S_2Cd$ group, moving charge density from the C−S bond toward the S−Cd bond (Scheme 3A). Second, the Lewis base solvent can serve as a protonated intermediate and facilitate the proton transfer required in the reaction (Scheme 3B). Third, it can ligand the cadmium (or metal, in general) (Scheme 3C), weakening at least one CdS bond in the dixanthate, activating it as a convenient leaving group and thus facilitating the formation of a full CdS bond. Finally the solvent can stabilize the particles (and the intermediate embryo cores) by forming a capping layer, as well as the xanthic acid. All these effects depend on the Lewis base nature of the solvent. It should be sufficiently strong to function as described above. However, it should not be too strong a ligand, so as not to block the adsorption and subsequent reaction of the metal xanthate.

SCHEME 3: Possible Ways of Involvement of a Lewis Base in the Decomposition of Cd−Xanthate (Z = Xanthate)

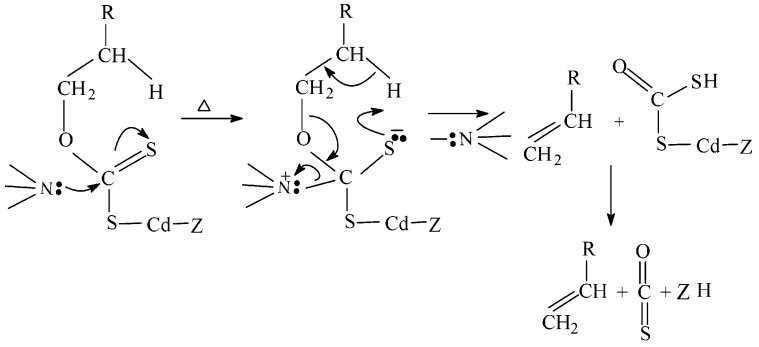

(A) Nucleophilic attack on the (thio) carbonyl center

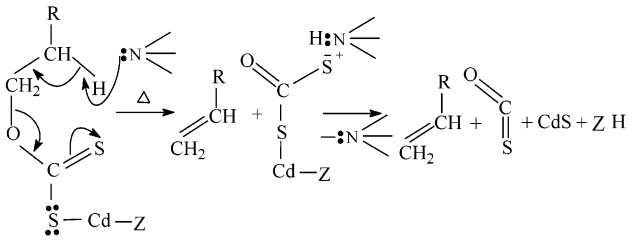

(B) Protonated intermediates

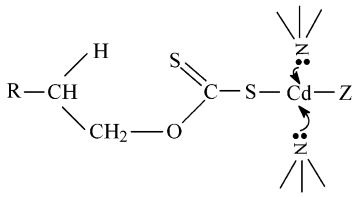

(C) Ligand stabilization of the metal center

SCHEME 4: PM3 Results for the Energy of Possible Species Involved in the Chugaev (A) and the Cadmium-Driven Chugaev-like Reaction (B)

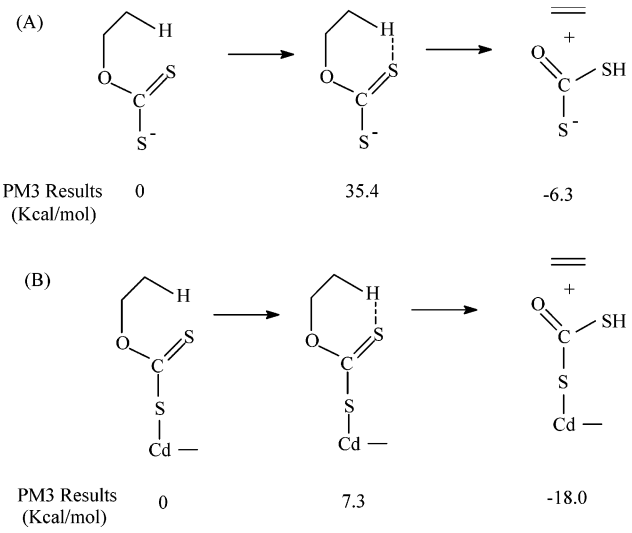

Full-scale density functional calculations are under way to validate the mechanism. Preliminary lower level calculations (MP3) indicate that indeed the intermediate in the decomposition of xanthate is strongly stabilized in the cadmium complex. The energy of the cadmium-stabilized possible intermediate (Scheme 4) is stabilized by 23−28 kcal/mol compared to the methyl thioester or the anion in the conventional Chugaev reaction.

The release of the OCS in the decomposition, as in the classical Chugaev reaction, irreversibly drives the reaction to completion, in addition to the irreversible nature of the CdS binding itself. Once a core of CdS (or other metal sulfide) forms, additional cadmium dixanthtae can attach to the surface of this core (or particle), replacing the amine and decomposing to extend the CdS lattice.

We measured the weight loss during the reaction of Cd−HDX in HDA, and it qualitatively corresponds to loss of OCS. As an example, 0.2 g of Cd−HDX in 1 g of HDA yielded after reaction 1.187 g of product and solvent (before precipitation). This is a residual of 86%, close to the expected remaining 92% after weight loss from evolution of OCS (some of the xanthate that did not react with Cd ions might also decompose).

3.6. Synthesis of Core/Shell CdS/ZnS Particles. As described in detail in the Experimental Section, core/shell CdS/ZnS structures are synthesized in a stepwise procedure with hexadecylxanthates of Cd and Zn as their precursors, with and without isolation of the core CdS particles. Here we present results for the production of CdS/ZnS particles with prior isolation of CdS particles. Shelling with ZnS is known to reduce and even eliminate the defect fluorescence of CdS. To emphasize this effect in the following set of experiments we do not fully anneal the CdS particles, synthesized from Cd−HDX at 70 °C (30min), and only briefly heat them up to 120 °C (for 10 min). The particles are isolated and dried at room temperature. Their solution in chloroform has a weak excitonic emission dominated by a broad surface trap PL band. The absorbance shows a shoulder with a band edge at 452 nm (curve a in Figure 11A,B).

The CdS cores are coated with ZnS in two stages, as described in the Experimental Section. One change we introduce here compared to the experimental is that the final temperature and the annealing at each stage is 160 °C. The reason for that will be made clear shortly; however, we note at present that the color of the solution remains yellow throughout. The absorbance band edge of the first stage of ZnS-treated particles shifts from 452 nm (of the bare CdS cores) to 440 nm, possibly indicating that CdS/ZnS core/shell particles are formed.

The emission spectrum now shows only a very small surface-trap broad peak, while the excitonic emission peak becomes much more intense and blue-shifts to 436 nm. This is a strong indication that indeed shelling takes place. Upon adding the

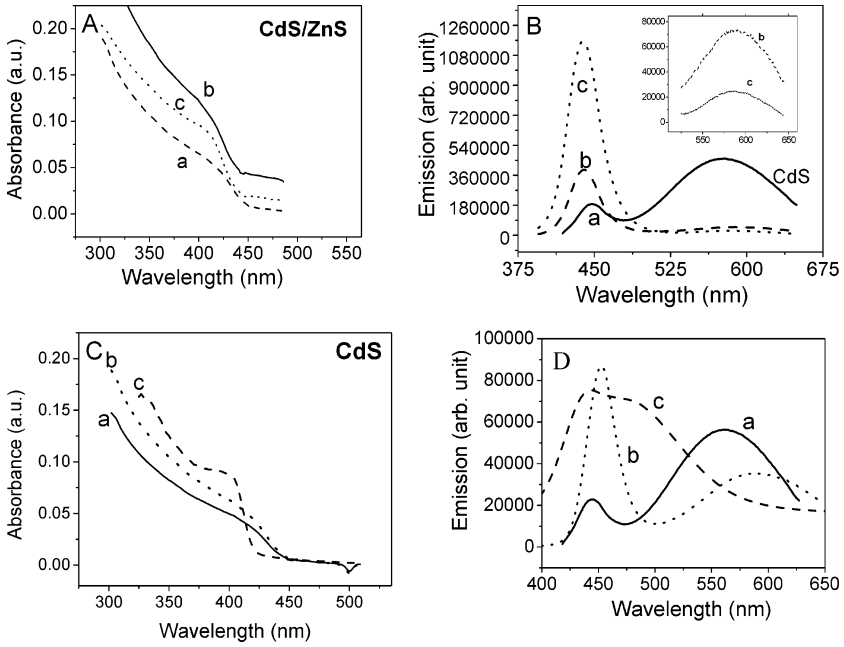

Figure 11. The UV−visible absorption (A) and PL (B) spectra of the two-step formation of CdS/ZnS core/shell particles: (curve a) nonshelled and un-annealed CdS particles; (curve b) the same CdS particles after one stage of coating with ZnS (produced form ZN−HDX); (curve c) the same CdS particles twice coated with ZnS. Insert in B: expanded view of the broad defect band of "b" and "c". Panels C and D are the UV−visible absorption and the PL spectra of a control: CdS particles treated in the same temperature and solution protocol, as in panels A and B, respectively, except that Zn−HDX was not used, i.e. the CdS particles are not shelled. The excitation is at 370 nm. Curves b and c in panel A were shifted upward for clarity. Both start from 0.0.

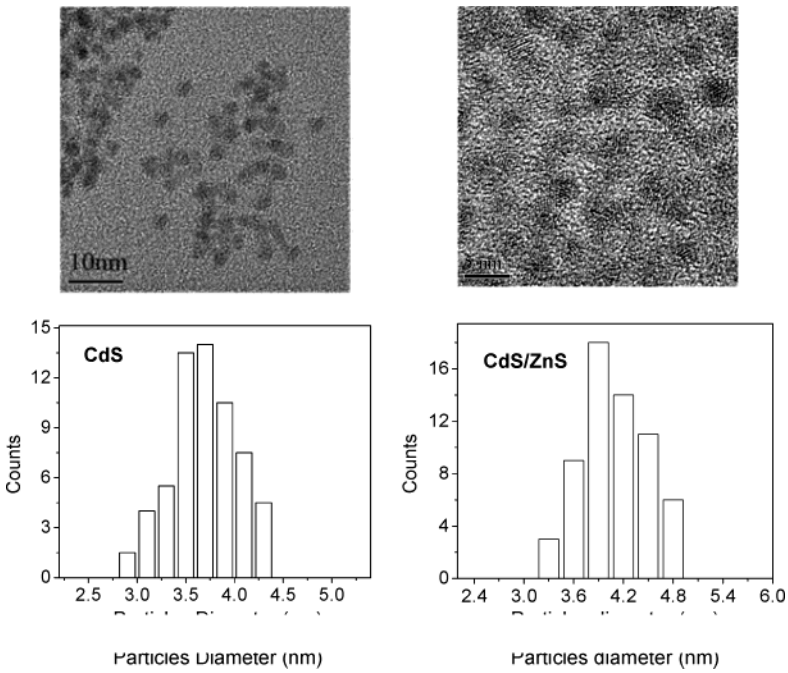

Figure 12. TEM micrograph and size distribution histograms of CdS (left) and core/shell CdS/ZnS particles (right) produced in a two-step process with a 1:2 molar ratio of Cd and Zn.

second batch of Zn−HDX and reacting it, the absorption and the emission bands do not show any further shift, though the excitonic emission becomes even more intense, with a concurrent decrease in the intensity of the broad, long wavelength fluorescence, (Figure 11B, inset). The QY of the excitonic band increases from much below 1% to ∼16% (with excitation at 370 nm).

As a control experiment we repeat the whole procedure exactly as described, except that we do not add any Zn−HDX (we add only HDA), preventing any coating of the CdS cores. Specifically, the same temperature protocol is applied, with final annealing at 160 °C. The results are summarized in Figure 11C,D. After the first (blank) heating cycle, to 120 °C, the absorption of the CdS particles does not change. This should be contrasted with the shift observed for the first stage ZnS-shelled particles. Furthermore, the excitonic emission band red-shifts by ∼10 nm, again contrary to the blue-shift of the shelled particles. Its intensity strongly increases (to QY ∼1.3%), in parallel with a decrease in the intensity of the long-wavelength emission. This is simple annealing, as we have shown previously.[35] Upon completing the second cycle and heating to 160 °C dramatic changes take place, in shear contrast to the very small changes that occur with the shelled particles (this is why we chose to go up to 160 °C). The absorption spectrum changes drastically, as is apparent even to the naked eye in the change of the color of the solution from yellow to orange-red. Similarly the emission spectrum changes entirely, exhibiting a broad dual peak in the 400−500 nm region, instead of the narrow excitonic (plus perhaps surface) emissions, resembling the emission spectrum of polygonal CdS, obtained previously at high temperature (curve c, Figure 11D).

As another comparison, we heat the ZnS-shelled CdS particles all the way up to 200 °C for prolonged times (>3 h). Yet, no changes in their spectra are observed. The shell evidently protects the CdS particles against changes at the high temperatures.

TEM micrographs, Figure 12, show that the Zn−HDX treated CdS particles (with 1:2 molar ratio Cd:Zn) are 4.1 ± 1 nm in diameter, while the initial CdS particles are ∼3.7 ± 0.7 nm, which corresponds to the size calculated from the band edge of the adsorption.[37] On the basis of the same analysis of the spectrum, with the threshold of absorption of the Zn-treated CdS particles being at 436 nm (curve c, Figure 11A,B), we calculate a particle diameter of ∼3 nm. This, of course, assumes that the particles are pure, uncoated CdS particles. Thus we see that by TEM the actual shelled particles are larger than the initial CdS cores, by 0.4 nm, and much larger than what is expected on the basis of the absorption spectrum of the (bare) particles. This is a strong indication that the CdS particles are indeed coated by a shell of ZnS. At the specific Zn:Cd molar ratio we used, $R =$ 2:1, a $d_{CdS} = 3.7$ nm diameter CdS particle should produce a $d = 4.3$ nm shelled particle (eq 2), very close to the 4.1 nm we measure by TEM. Actually this agreement is a bit surprising considering the uncertainty in the sizes.

The diameter of the shelled particle, d, is calculated from eq 2

$$d = [1 + R(\rho_{CdS}/\rho_{ZnS})(MW_{ZnS}/MW_{CdS})]^{1/3} d_{CdS} \qquad (2)$$

with ρ being the density of the sulfides (4.82 g/cm^3 and 4.1 g/cm^3 for CdS and ZnS, respectively), MW the molecular weight of the metal sulfide, d_{CdS} the diameter of the bare CdS core (3.7 nm), and R the Zn:Cd molar ratio.

Summarizing this part, we produce CdS/ZnS core/shell particles. We demonstrate this by the behavior of the absorption and emission spectra (band positions, band shapes, and intensities), their temperature dependence and the results of TEM, together with simple theoretical modeling. The shell is produced in exactly the same manner as the core. The shell eliminates the broad surface emission and very significantly increases the quantum yield of the narrow excitonic band. In addition, the insensitivity to the precise synthesis protocol (one- vs two-stage synthesis, temperature protocol, etc.), especially with low-temperature synthesis (as low as 60 °C), is, we believe, an indication that core/shell structures form rather than mixed particles.

3.7. Synthesis of Core/Shell ZnS/CdS Particles. Here we demonstrate the versatility of our methods in the production of

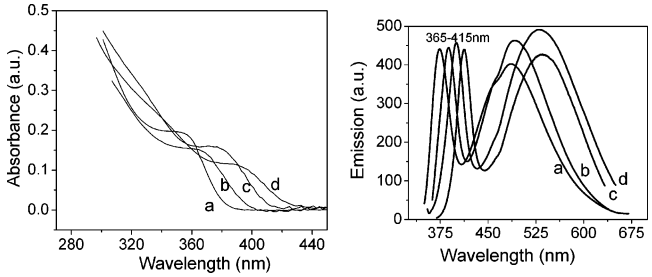

Figure 13. Absorption (left) and emission (right) spectra of particles formed from a mixture of Zn−HDX and Cd−HDC in HDA at 120 (a), 140 (b), 170, (c), and 210 °C (d). PL excitation was at 370 nm.

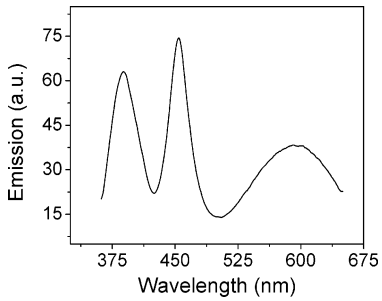

Figure 14. PL spectra of ZnS/CdS in the presence of excess Cd−HDC (5×10^{-4} mol). PL excitation was at 370 nm.

ZnS/CdS core/shell structures. These are of interest as intermediates in the production of core/shell/shell structures (quantum-dot-quantum-wells). Furthermore, as we show here, they exhibit an interesting spectral behavior. In the single loading synthesis, we use a combined HDA solution of Zn−HDX that reacts at a low temperature, <100 °C, and Cd−HDC, which, by itself in HDA, requires a higher temperature for reaction to take place, >140 °C. The procedure is described in detail in the Experimental Section.

The main point is first to form ZnS cores from Zn−HDX at low temperature, and then to heat these cores to a higher temperature, but below that required for the Cd−HDC reaction by itself. Because of the presence of the ZnS cores CdS starts to form from Cd−HDC just above 100 °C, but only on the ZnS cores, shelling them. Cd−HDC cannot react at this temperature in the bulk and thus it cannot form separate CdS particles (which have mostly broad defect PL).

While separate CdS particles obtained from Cd−HDC in HDA (at a higher temperature) give an absorption shoulder above 430 nm (Figure 6), we find in our core/shell synthesis a clear absorbance peak as low as 360 nm (Figure 13). When the reaction temperature is gradually increased from 140 °C to 210 °C, the position of the UV−visible absorption band gradually shifts from 360 nm to 400 nm. Similarly the corresponding ~40 nm fwhm (excitonic) emission band shifts from 365 nm to 415 nm (Figure 13) and the broad (surface defect) band also shifts from 480 nm to 525 nm. Apparently the CdS forms only on the ZnS cores as a thin shell or in the form of clusters, as evidenced from the absence of any emission above 430 nm, characteristic of separate CdS particles. At first sight our spectra resemble those observed by Spanhel et al.[43] and which they attributed to co-colloid ZnS−CdS particles. However, their procedure reacted mixtures of the cadmium and the zinc salts with H_2S, without any precautions to avoid coprecipitation of both metals. In our procedure, first ZnS cores form, and only at a higher temperature the cadmium precursor reacts. Furthermore, when we use larger amounts of Cd−HDC (3.5×10^{-4} mol compared to 7.1×10^{-5} mol) the absorption peak shifts up to 420 nm, and the usual excitonic emission is observed at 450 nm (in addition to the 380 nm emission), indicating the presence of separate CdS particles in solution, or of thick shells of CdS (Figure 14).

In a separate sequential experiment we first produce ZnS particles (from Zn−HDX), precipitate, and wash them. These ZnS particles are suspended in HDA with Cd−HDX and heated to below 135°C (Zn:Cd molar ratio of 1:1.5). Under these circumstances, we finally observe an unusually sharp absorption peak at 364 nm and a narrow (35 nm fwhm) CdS excitonic emission at ~410 nm (Figure 15). Since we do not observe from these samples excitonic emission above 430 nm, indicative of separate CdS particles, it is clear that the PL is coming from ZnS particles fully or partially coated with CdS, as expected from the fully sequential nature of this procedure. This finding confirms that also in the single-pot, two-stage procedure described above, we likewise obtain ZnS particles coated with CdS (complete?) shells or clusters. Thus, we do not believe that the co-colloids produced by Spanhel et al.[43] are the same as ours (though perhaps one should study their procedure in more detail to substantiate this).

Summary

We presented here a detailed study of the production of metal sulfide particles via a single precursor, xanthate-based procedure, employing an alkyl amine Lewis base solvent. This approach offers a great deal of control of the size and the shape of the particles and facilitates their production at relatively low temperatures (even below room temperature, for some metals) under ambient conditions, without need of glovebox practices. Despite the low temperature the particles are crystalline and are easily annealed or shelled to eliminate optical transitions originating from (surface) defects and traps. The excitonic emission (for CdS) is narrow and tunable. What appears to be core/shell structures are formed in the same general method by using single- or two-step procedures, achieving high PL quantum

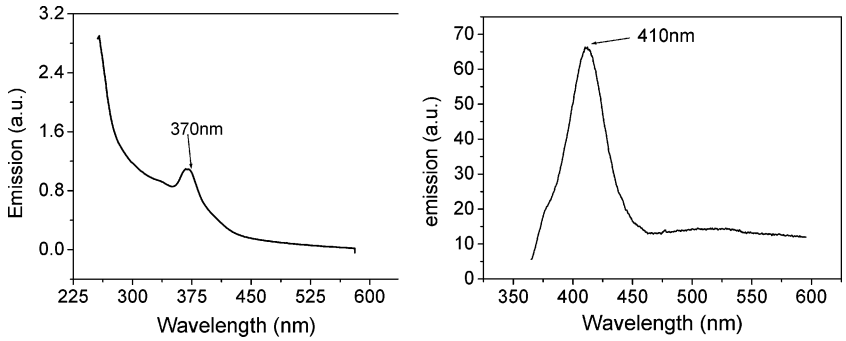

Figure 15. UV−visible (left) and PL (right) spectra of ZnS/CdS particles synthesized from ZnS and Cd−HDX in HDA with isolation of ZnS. PL excitaton was at 370 nm.

yields. A high energy excitonic emission at or below 415 nm is observed for CdS deposited in the presence ZnS particles.

Acknowledgment. We thank V. Khodorkovsky for the results of the preliminary MP3 calculation and J. Klug for help with the xanthates.

References and Notes

(1) Brus, L. E. *J. Chem. Phys.* **1986**, *90*, 2555.
(2) Alivisatos, A. P. *Science* **1996**, *271*, 933.
(3) Qu, L.; Peng, X. *J. Am. Chem. Soc.* **2002**, *124*, 2049.
(4) Goldman, E. R.; Balighian, E. D.; Mattoussi, H.; Kuno, M. K.; Mauro, J. M.; Tran, P. T.; Anderson, G. P. *J. Am. Chem. Soc*. **2002**, *124*, 6378.
(5) Mattoussi, H.; Mauro, J. M.; Goldman, E. R.; Anderson, G. P.; Sundar, V. C.; Mikulec, F. V.; Bawendi, M. G. *J. Am. Chem. Soc*. **2000**, *122*, 12142.
(6) Mingyong, H.; Xiaohu, G.; Jack, Z. S.; Shuming, N. *Nat. Biotechnol*. **2001**, *19*, 631.
(7) Jaiswal. J. K.; Mattoussi, H.; Matthew M. J.; Simon, S. M. *Nature Biotechnol*. **2003**, *21*, 47.
(8) Bruchez, M.; Moronne, M.; Gin, P.; Weiss, S.; Alivisatos, A. P. *Science* **1998**, *281*, 2013.
(9) Chan, W. C.; Nie, S. *Science* **1998**, *281*, 2016.
(10) Nirmal, M.; Brus, L. *Acc. Chem. Res.* **1999**, *32*, 407.
(11) Empedocles, S. A.; Bawendi, M. G. *J. Phys. Chem. B* **1999**, *103*, 1826.
(12) Manna, L.; Scher, E. C.; Li, L. S.; Alivisatos, A. P. *J. Am. Chem. Soc.* **2002**, *124*, 7136.
(13) Logunov, S.; Green, T.; Marguet, S.; El-Sayed, M. A. *J. Phys. Chem. A* **199**8, *102*, 5652.
(14) Haesselbarth, A.; Eychmueller, A.; Weller, H. *Chem. Phys. Lett.* **1993**, *203*, 271.
(15) Wu, F.; Zhang, J. Z.; Kho, R.; Mehra, R. K. *Chem. Phys. Lett.* **2000**, *330*, 237.
(16) Chestnoy, N.; Harris, T. D.; Hull, R.; Brus, L. E. *J. Phys. Chem*. **1986**, *90*, 3393.
(17) Murray, C. B.; Norris, D. J.; Bawendi, M. G. *J. Am. Chem. Soc.* **1993**, *115*, 8706.
(18) Peng, X. G.; Schlamp, M. C.; Kadavanich, A. V.; Alivisatos, A. P. *J. Am. Chem. Soc.* **1997**, *119*, 7019.
(19) Mattoussi, H.; Radzilowski, L. H.; Dabbousi, B. O.; Thomas, E. L.; Bawendi, M. G.; Rubner, M. F. *J. Appl. Phys.* **1998**, *83*, 7965.
(20) Manna, L.; Scher, E. C.; Alivisatos, A. P. *J. Am. Chem. Soc*. **2000**, *122*, 12700.
(21) Peng, X. G.; Manna, L.; Yang, W. D.; Wickham, J.; Scher, E. C.; Kadavanich, A.; Alivisatos, A. P. *Nature* **2000**, *404*, 59.
(22) Peng, Z. A.; Peng, X. *J. Am. Chem. Soc.* **2001**, *123*, 183.
(23) Yu, W.; Peng, X. *Angew. Chem., Int. Ed*. **2002**, *41*, 2368.
(24) Joo, J.; Na, H. B.; Yu, T.; Yu, J. H.; Kim, Y. W.; Wu, F.; Zhang, J. Z.; Hyeon, T. *J. Am. Chem. Soc.* **2003**, *125*, 11100.
(25) O'Brien, P.; Zhang, X.; Motevalli, M. *J. Mater. Chem.* **1997**, *7*, 1011.
(26) Nair, P. S.; Radhakrishnan, T.; Revaprasadu, N.; Kolawole, G. A. O'Brien, P. *Chem. Commun.* **2002**, 564.
(27) Green, M.; O Brien, P. *Chem. Commun.* **1998**, 2459.
(28) Ludolph, B.; Malik, M.; O'Brien, P.; Revaprasadu, N. *Chem. Commun.* **1998**, 1849.
(29) Green, M.; O'Brien, P. *J. Mater. Chem.* **1999**, *9*, 243.
(30) Revaprasadu, N.; Malik, M. A.; O'Brien, P.; Wakefield, G. *Chem. Commun.* **1999**, 1573.
(31) Lazell, M.; O'Brien, P. *Chem. Commun.*, **1999**, 2041.
(32) Green, M.; O'Brien, P. *Chem. Commun.*, **1999**, 2235.
(33) Malik, M. A.; Revaprasadu N.; O'Brien, P. *Chem. Mater*. **2001**, *13*, 913.
(34) Pickett, N. L.; O'Brien, P. *Chem. Rec.* **2001**, *1*, 467.
(35) Kortan, A. R.; Hull, R.; Opila, R. L.; Bawendi, M. G.; Steigerwald, M. L.; Carroll, P. J.; Brus, L. E.; Quinlan, F. T.; Kuther, J.; Tremel, W.; Knoll, W.; Risbud, S.; Stroeve, P. *Langmuir* **2000**, *16*, 4049.
(36) Gaponik, N.; Talapin, D. V.; Rogach, A. L.; Eychmuller, A.; Weller, H. *Nano Lett.* **2002**, *2*, 803.
(37) Pradhan, N.; Efrima, S. *J. Am. Chem. Soc.* **2003**, *125*, 2050.
(38) Sawant, P.; Kovalev, E.; Klug, J. T.; Efrima, S. *Langmuir* **2001**, *17*, 1913.
(39) Glass, R. S.; Petsom, A.; Hojjatie, M.; Coleman, B. R.; Duchek, J. R.; Klug, J.; Wilson, G. S. *J. Am. Chem. Soc.* **1988**, *110*, 4772.
(40) Schonberg, A.; Wagner, A. In *Methoden der Organischen Chemie (Houben-Weil);* Thieme: Stuttgart, Germany, 1954; Vol. 9.
(41) Olmsted, J. *J. Phys. Chem*. **1979**, *83*, 2581.
(42) O'Neil, M.; Marohn, J.; McLendon, G. *J. Phys. Chem*. **1990**, *94*, 4356.
(43) Spanhel, L.; Haase, M.; Weller, H.; Henglein, A. *J. Am. Chem. Soc.* **1987**, *109*, 5649.
(44) Chestnoy, N.; Harrs, T. D.; Hull, R.; Brus, L. E. *J. Phys. Chem.* **1986**, *90*, 3393.
(45) International Center for Diffraction Data, 1997.
(46) Cheon, J.; Zink, J. *J. Am. Chem. Soc*. **1997**, *119*, 3838.
(47) Nair, P. S.; Radhakrishnan, T.; Revaprasadu, N.; Kolawole, G.; O'Brien, P. *J. Mater. Chem.* **2002**, *12*, 2722.
(48) Jun, Y.; Lee, S. M.; Kang, N. J.; Cheon, J. *J. Am. Chem. Soc*. **2001**, *123*, 5150.
(49) De Puy, C. H.; King, R. W. *Chem. Rev.* **1960**, *60*, 431.